V European Conference on Computational Fluid Dynamics
ECCOMAS CFD 2010
J. C. F. Pereira and A. Sequeira (Eds)
Lisbon, Portugal,14-17 June 2010

A SIMPLE NVD/TVD-BASED UPWINDING SCHEME FOR CONVECTION TERM DISCRETIZATION

Giseli A. B. Lima*, **Laís Corrêa***, **Miguel A. C. Candezano***, **Patrícia Sartori*** **and Valdemir G. Ferreira***

*Universidade de São Paulo,
Av. Trabalhador São-Carlense, 400, São Carlos-SP
e-mail: giabl, lacorrea, mcaro, psartori, pvgf@icmc.com.br

Key words: High Resolution Schemes, Upwinding, Convection Term, Conservation Laws, Navier-Stokes Equations

Abstract. *The correct modeling for processes involving convection, without introducing excessive artificial damping while retaining high accuracy, stability, boundedness and simplicity of implementation continues being nowadays a challenging task for the scientific CFD community. In this context, the objective of this study is to present and to evaluate the performance of a new TVD-based upwinding scheme, namely Six-Degree Polynomial Upwind Scheme of* C^1 *Class (SDPUS-C1), for convection term discretization. SDPUS-C1 satisfies the TVD principle of Harten and is based on the NVD formulation of Leonard. Firstly, a description of the scheme is done and then numerical results are presented for two-dimensional hyperbolic conservation laws, such as acoustics, Burgers and Euler equations. Finally, as application, the SDPUS-C1 scheme is used for the computational simulation of three-dimensional incompressible fluid flows involving moving free surfaces.*

1 INTRODUCTION

The numerical solution of fluid flow problems has emerged as a viable alternative to both experimental and analytical studies. In order to make the simulations of these problems more acceptable and reliable, there is an increasing demand for development, analysis and implementation of a upwinding convective scheme (in general nonlinear) for solving complex flow phenomena which offers simplicity, accuracy, robustness and versatility. Such a scheme is particularly important when one wants to simulate transient incompressible flows at high values of Reynolds number and with moving free surfaces.

In the literature there are a variety of schemes to approximate convective terms. For instance, first order upwind schemes, such as FOU[3], are unconditionally stable, but they have a diffusive character that, in general, smoothing the solution. On the order hand, classical high resolution schemes, such as central differences[4] schemes, such as the Lax-Wendroff[4], the QUICK[11] scheme (and its related QUICK with estimated stream terms - QUICKEST) can often produce unphysical oscillations which, most of the time, can lead to numerical instability.

In this work, we presented a new high resolution scheme, namely Six-Degree Polynomial Upwind Scheme of C^1 Class (SDPUS-C1), for the discretization of the linear and nonlinear convection terms. The scheme is based on the NVD formulation of Leonard[11] and satisfies the TVD[9] and CBC[8] stability criteria. Firstly, a description of the scheme is done and then numerical results are presented for two-dimensional hyperbolic conservation laws (acoustics, Burgers and Euler equations). Finally, as application, the SDPUS-C1 scheme is used for the computational simulation of three-dimensional incompressible fluid flows involving moving free surfaces. The numerical results show that this new polynomial upwind convection scheme performs very well.

2 NORMALIZED VARIABLE AND STABILITY CRITERIA

Before proceeding to the derivation of the SDPUS-C1 convective scheme, it is essential to present the normalized variables (NV) of Leonard[11] and, using the convection boundedness criterion (CBC) of Gaskell and Lau[8] and total variation diminishing (TVD) constraint of Harten[9], the conditions required for the construction of a monotonic upwinding scheme.

In order to interpolate the numerical flux ϕ_f at a boundary face f between two control volumes, we will use three neighboring grid points, namely D (Downstream), U (Upstream) and R (Remote-upstream), labeled according to the local wind direction (upwinding) V_f (see figure 1). For multidimensional problems, this strategy is applied in the same fashion, with each convective derivative approximated along of the relevant variable (direction-by-direction). In summary, the scheme is given by

$$\phi_f = (\phi_D, \phi_U, \phi_R). \tag{1}$$

To simplify the functional relationship given by equation (1), the original variables are

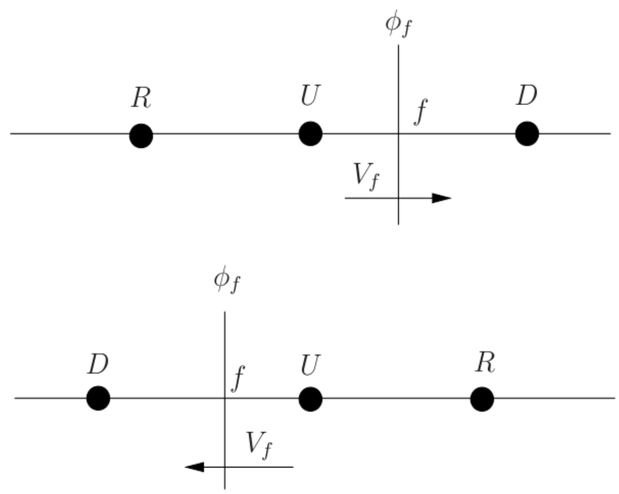

Figure 1: Interfaces and their related grid points for determining an upwinding scheme.

transformed in NV as

$$\hat{\phi}_{[\ \ ]} = \frac{\phi_{[\ \ ]} - \phi_R}{\phi_D - \phi_R}. \tag{2}$$

The advantage of this new formulation is that the interface value $\hat{\phi}_f$ depends of $\hat{\phi}_U$ only, since $\hat{\phi}_D = 1$ and $\hat{\phi}_R = 0$. Thus, equation (1) can be rewritten as

$$\hat{\phi}_f = \hat{\phi}_f(\hat{\phi}_U). \tag{3}$$

The normalized variable diagram (NVD) was proposed by Leonard[11] and is based on the definition (2) and on the functional relationship (3). According to Leonard[11], for $0 \leq \hat{\phi}_U \leq 1$, it is possible to derive a nonlinear monotonic third order NV scheme by imposing the following conditions: $\hat{\phi}_f(1) = 1$ (a necessary condition); $\hat{\phi}_f(0) = 0$ (a necessary condition); $\hat{\phi}_f(1/2) = 3/4$ (a necessary and sufficient condition to reach second order of accuracy); and $\hat{\phi}'_f(1/2) = 3/4$ (a necessary and sufficient condition to reach third order of accuracy). Leonard[11] also recommends that, for values of $\hat{\phi}_U < 0$ or $\hat{\phi}_U > 1$, the scheme must be extended in a continuous manner using the FOU[3] scheme.

Gaskell and Lau[8] (see also Waterson and Deconinck[18]) proposed the CBC, which is a necessary and sufficient condition for a scheme possessing boundedness, namely:

$$\begin{cases} \hat{\phi}_U \leq \hat{\phi}_f(\hat{\phi}_U) \leq 1 & \text{if} \quad \forall \hat{\phi}_U \in [0,1]; \\ \hat{\phi}_f = \hat{\phi}_f(\hat{\phi}_U) = \hat{\phi}_U & \text{if} \quad \forall \hat{\phi}_U \notin [0,1]; \\ \hat{\phi}_f(1) = 1 & \text{and} \quad \hat{\phi}_f(0) = 0. \end{cases} \tag{4}$$

These conditions determine the CBC region (see figure 2).

Another important convective stability criterion is the TVD constraint of Harten[9], which is a purely scalar property and ensures that spurious oscillations are removed from the numerical solution. In summary, considering a sequence of discrete approximations $\phi(t) = \phi_i(t)_{i\in\mathbb{Z}}$ to a scalar, the total variation (TV) at time t of this sequence is defined by

$$TV(\phi(t)) = \sum_{i\in\mathbb{Z}} |\phi_{i+1}(t) - \phi_i(t)|. \tag{5}$$

Then, the scheme is TVD if the following condition is satisfied:

$$TV(\phi^{n+1}) \leq TV(\phi^n), \quad \forall n \in \mathbb{N}. \tag{6}$$

With the considerations and concepts introduced by Harten[9], Sweby[16] defined, in the context NVD, the set of restrictions

$$\begin{cases} \hat{\phi}_f \in [\hat{\phi}_U, 2\hat{\phi}_U] \ \text{ and } \ \hat{\phi}_f \leq 1, & \text{if} \quad \hat{\phi}_U \in [0,1], \\ \hat{\phi}_f = \hat{\phi}_U, & \text{if} \quad \hat{\phi}_U \notin [0,1], \end{cases} \tag{7}$$

which led the TVD region (see figure 2).

After one developed a NVD/TVD-based upwind scheme, we derive the associated flux-limiter by rewriting the original scheme in the following way (see Sweby[16] and Waterson and Deconinck[18]):

$$\hat{\phi}_f = \hat{\phi}_U + \frac{1}{2}\psi(r)(1 - \hat{\phi}_U), \tag{8}$$

where $\psi(r)$ is the flux-limiter that determines the level of antidifusividade, r being a local shock sensor given by ratio of consecutive gradients as

$$r = \frac{\left(\dfrac{\partial \phi}{\partial x}\right)_g}{\left(\dfrac{\partial \phi}{\partial x}\right)_f}. \tag{9}$$

On uniform meshes, it is given by

$$r = \frac{\phi_U - \phi_R}{\phi_D - \phi_U} \tag{10}$$

and in NV is

$$r = \frac{\hat{\phi}_U}{1 - \hat{\phi}_U}. \tag{11}$$

In addition, the TVD concept was translated by Sweby[16] into a set of limitations for dictating the behavior of the flux-limiter function, that is

$$\begin{cases} \psi(r) = 0, & \text{if} \quad r \leq 0, \\ 0 \leq \psi(r) \leq \min\{2, 2r\}, & \text{if} \quad r > 0. \end{cases} \tag{12}$$

In summary, figure 2 presents the regions for the three stability criteria discussed above (see equations (4), (7) and (12)).

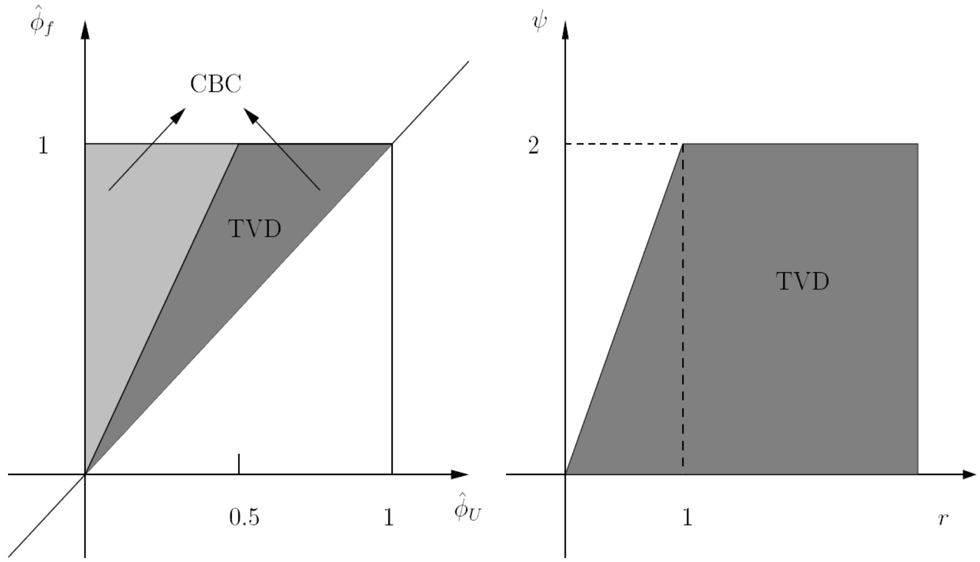

Figure 2: Regions for stability criteria: CBC and TVD regions (left) ; and flux-limiter region (right).

3 A BRIEF DESCRIPTION OF THE SDPUS-C1 SCHEME

In this section, we derive the SDPUS-C1 scheme by assuming that the NV at the cell interface f, $\hat{\phi}_f$, are related to $\hat{\phi}_U$ as a six-degree polynomial function of the form

$$\hat{\phi}_f = \sum_{k=0}^{6} b_k \hat{\phi}_U^k, \tag{13}$$

for $0 \leq \hat{\phi}_U \leq 1$, and a linear function (the FOU scheme), given by

$$\hat{\phi}_f = \hat{\phi}_U \tag{14}$$

for $\hat{\phi}_U < 0$ or $\hat{\phi}_U > 1$.

In equation (13), we set a free parameter (say $b_2 = \gamma$) and determine the other coefficients by imposing the four conditions of Leonard[11] outlined above plus the condition of continuous differentiability for $\hat{\phi}_f = \hat{\phi}_f(\hat{\phi}_U)$ on the whole remains, in another works the equations (13) and (14) are linked on the points $(0, 0)$ and $(1, 1)$ with the same values for the first derivatives. Thus, the SDUPS-C1 scheme is a continuously differentiable function. And it is important to note here that, according to Lin and Chieng[14], if this property is not satisfied then convergence problems may be found in unsteady calculations when large time steps are employed.

In summary, the convection upwind SDPUS-C1 scheme is given by

$$\hat{\phi}_f = \begin{cases} (-24+4\gamma)\hat{\phi}_U^6 + (68-12\gamma)\hat{\phi}_U^5 + (-64+13\gamma)\hat{\phi}_U^4 + (20-6\gamma)\hat{\phi}_U^3 + \gamma\hat{\phi}_U^2 + \hat{\phi}_U, & \hat{\phi}_U \in [0,1], \\ \hat{\phi}_U, & \hat{\phi}_U \notin [0,1], \end{cases} \tag{15}$$

In the same way as was done by Ferreira et al.[6,7], the corresponding flux-limiter function for the SDPUS-C1 scheme is derived by combining the equations (15), (8) and (11) to obtain

$$\psi(r) = \begin{cases} \dfrac{(-8+2\gamma)r^4 + (40-4\gamma)r^3 + 2\gamma r^2}{(1+r)^5}, & r \geq 0, \\ 0, & r < 0. \end{cases} \tag{16}$$

The flux-limiter (16) can be also written, in a more widely used notation (see, e.g., Waterson and Deconinck[18]), as

$$\psi(r) = \max\left\{0, \ \frac{0.5(|r|+r)((-8+2\gamma)r^3 + (40-4\gamma)r^2 + 2\gamma r}{(1+|r|)^5}\right\}. \tag{17}$$

It is important to observe that the SDPUS-C1 scheme is nonlinear and combines boundedness with third order of accuracy. In particular, this scheme is TVD for $\gamma \in [4, 12]$ (see figure 3) and, consequently, is CBC. The flux-limiter function is depicted in the same figure. In this work, we considered $\gamma = 12$ because, for this value, the scheme is TVD and presented the best results (see Lima[13]).

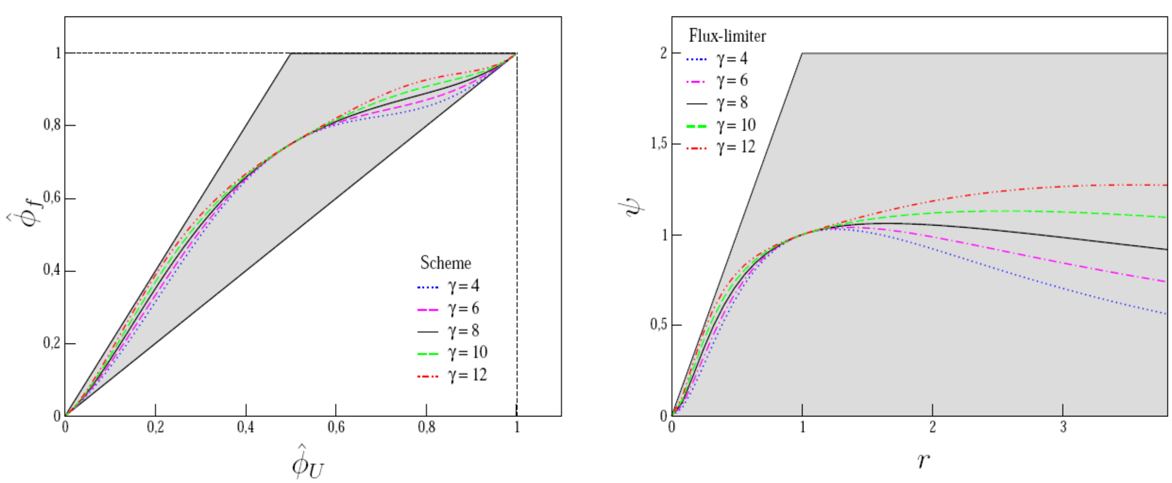

Figure 3: SDPUS-C1 scheme: TVD region (left) and flux-limiter region (right).

4 NUMERICAL RESULTS

In order to demonstrate the behavior, validity, flexibility and robustness of the SDPUS-C1 scheme, in this section problems formulated by conservation laws will be solved. Comparison with reference solutions is initially assessed. The SDPUS-C1 scheme is then used to solve three-dimensional incompressible Navier-Stokes equations involving moving free surface.

4.1 Conservation laws

Many problems in science and engineering involve quantities that are preserved and that lead to certain types of partial differential equations called hyperbolic conservation laws. These laws are generally nonlinear and time-dependent. In the two-dimensional case, they are defined by

$$\frac{\partial \phi}{\partial t} + \frac{\partial F(\phi)}{\partial x} + \frac{\partial G(\phi)}{\partial y} = 0, \tag{18}$$

where $\phi = \phi(x, y, t) : \mathbb{R}^2 \times \mathbb{R} \to \mathbb{R}^m$ is the m-dimensional vector of the conservation variables and $F(\phi) = F(\phi(x, y, t)),\quad G(\phi) = G(\phi(x, y, t)) : \mathbb{R}^m \to \mathbb{R}^m$ are flux functions. Here we consider three particular cases these laws, namely: acoustics, Burgers and Euler equations. In order to resolve these equations, we have been used the well established CLAWPACK (Conservation LAW PACKage) code of LeVeque[12], which employs the finite volume methodology combined with the SDPUS-C1 flux-limiter (16).

4.1.1 Acoustics equations

The acoustics equations are formulated by the equation (18), with the vector of the conservation variables given by $\phi = [p, u, v]^T$ and flux functions by $F(\phi) = [Ku, p/\rho, 0]^T$ and $G(\phi) = [Kv, 0, p/\rho]^T$. $[u, v]^T$ is the velocity vector, and K, ρ and p are bulk modulus of compressibility of the material, density and pressure, respectively (for details, the reader is referred to LeVeque[12]). This system is solved in the domain $\Omega = [0, 1] \times [0, 1]$, where the interface $x = 0.5$ separates two materials (one on the left and another on the right) with density ρ and sound speed c given by $\rho_L = 1$, $c_L = 1$, and $\rho_R = 4$, $c_R = 0.5$. Another data for the simulation is the pulse for the pressure which leads to a radially-symmetric disturbance, namely

$$r = \sqrt{(x - 0.25)^2 + (y - 0.4)^2}. \tag{19}$$

The initial conditions are

$$p_0 = \begin{cases} 1 + 0.5\left[\cos\left(\frac{\pi \cdot r}{0.1}\right) - 1\right], \text{ if } & r < 0.1, \\ 0, & \text{otherwise,} \end{cases} \qquad u_0 = 0, \quad v_0 = 0 \tag{20}$$

and zero-order extrapolation on the boundary.

For the simulation of this problem, we consider as reference solution the Godunov method with the correction term containing the MC (Monotonized central-difference) flux-limiter. The numerical solution is obtained with this same method but using the SDPUS-C1 scheme as flux-limiter. For the numerical computation, we used a mesh size of 200×200 computational cells, and for the reference solution we employed a mesh size of 400×400 computational cells. In both the calculations, the Courant number was set as $\theta = 0.8$.

Figure 4 shows the cross-section from the simulation of the pressure at $t = 0.1$ and $t = 0.4$. One can observe from this figure that when the pressure pulse hits the interface, it is partially reflected and partially transmitted. From the same figures, the SDPUS-C1 scheme provides results in good agreement with reference solutions. In order to complete the analysis, we calculated the pressure variation as a function of distance from the origin (ie, p in $y = 0$), as shown in figure 5, which compares the SDPUS-C1 scheme with the reference solution, showing that the new scheme has good performance.

4.1.2 Burgers equation

The Burgers equation corresponds to the equation (18) with the vector of the conservation variables given by $\phi = u$ and flux functions $F(\phi) = G(\phi) = \frac{1}{2}u^2$. Here u is the velocity vector. This system is solved in $\Omega = [0, 1] \times [0, 1]$, supplemented with the piecewise constant initial data

$$u_0 = \begin{cases} 1, & \text{if} \quad 0.1 < x < 0.6 \quad \text{and} \quad 0.1 < y < 0.6, \\ 0.1 & \text{if} \quad \text{otherwise} \end{cases} \tag{21}$$

and periodic boundary conditions.

For the simulation of this hyperbolic system, the reference solution was obtained on a mesh size of 100×100 computational volumes using the Godunov method with the term correction employing the van Leer flux-limiter (see LeVeque[12]). The numerical solution was calculated by SDPUS-C1 scheme generated on a uniform mesh of 50×50 finite volumes. In both cases (numerical and reference), we considered $\theta = 0.8$. In figure 6, it is depicted the reference and numerical solutions for the u component at $t = 0.5$ and $t = 1$. It is possible to see from this figure that the SDPUS-C1 scheme presented good results.

4.2 Euler equations

In this section, we consider an inviscid, compressible and non-heat conducting gas modeled by Euler equations. These equations are given by (18), where $\phi = [\rho, \rho u, \rho v, E]^T$ is the vector of conserved quantities, $\mathbf{F}(\phi) = [\rho, \rho u^2 + p, \rho uv, (E + p)u]^T$ and $\mathbf{G}(\phi) = [\rho v, \rho uv, \rho v^2 + p, (E + p)v]^T$ are flux functions; being ρ, u, v, ρu, ρv, E and p the density, the x-velocity, the y-velocity, the x-momentum, the y-momentum, the total energy and the pressure, respectively. In order to close the system, the ideal gas equation of state $p = (\gamma - 1)(E - \frac{1}{2}\rho(u^2 + v^2))$ with $\gamma = 1.4$, was considered.

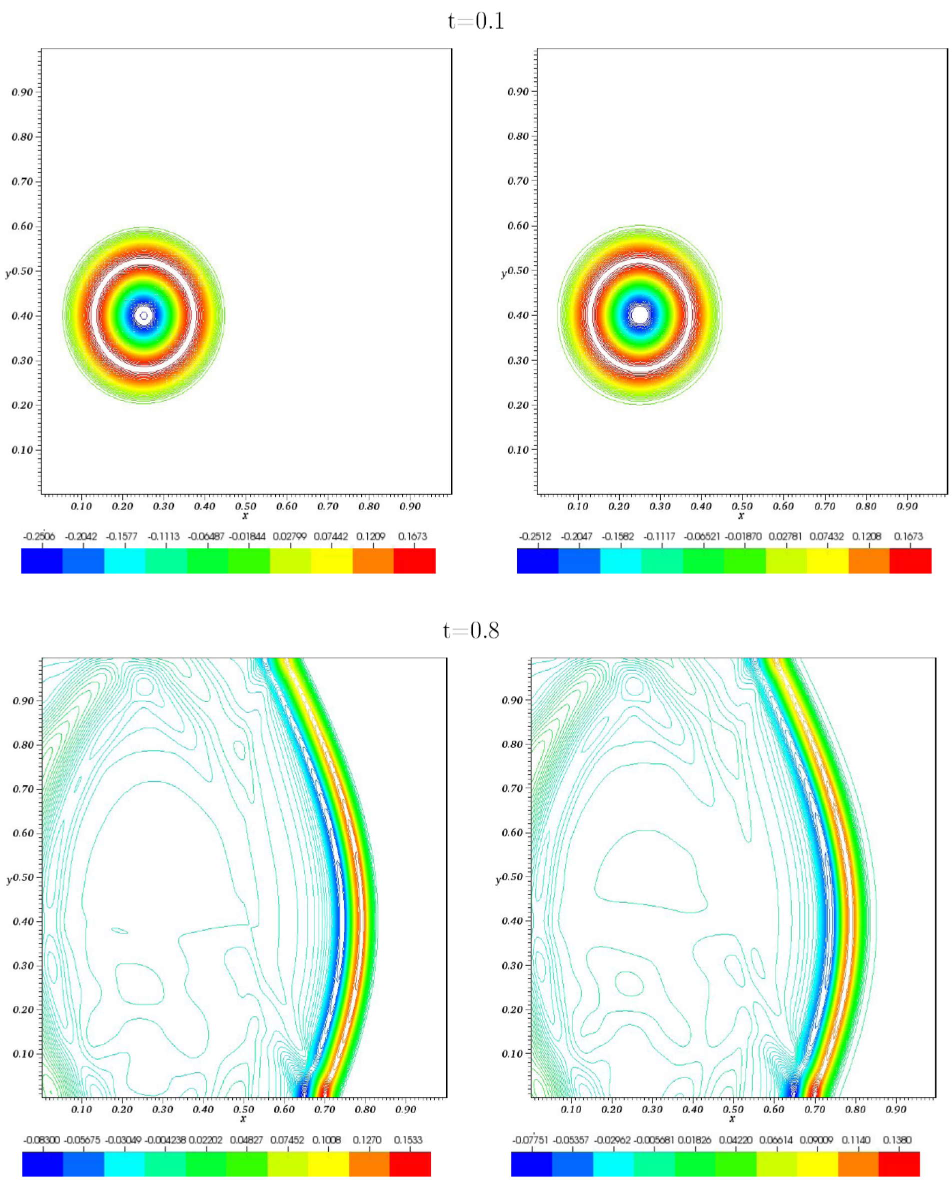

Figure 4: Numerial results for acoustics equation (cross-section from the simulation of the pressure): reference solution (left) and SDPUS-C1 scheme (right).

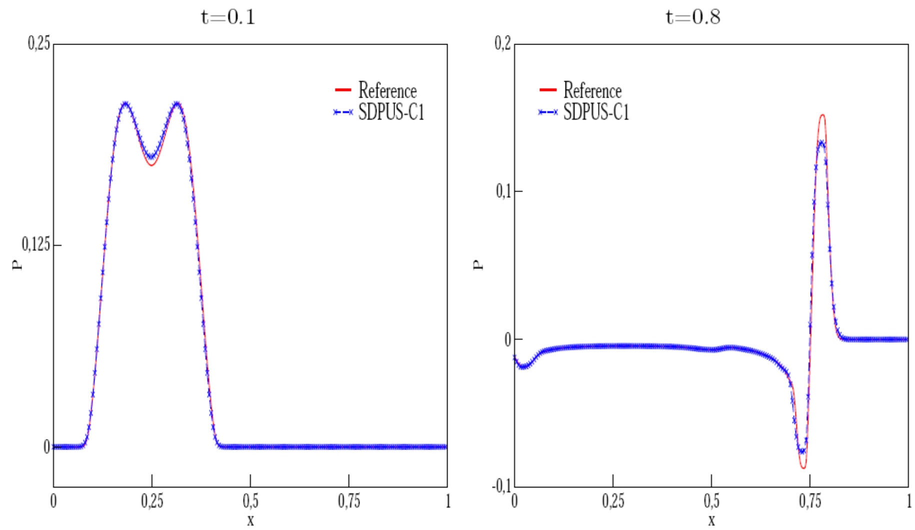

Figure 5: Numerial results for acoustics equation (p in $y = 0$).

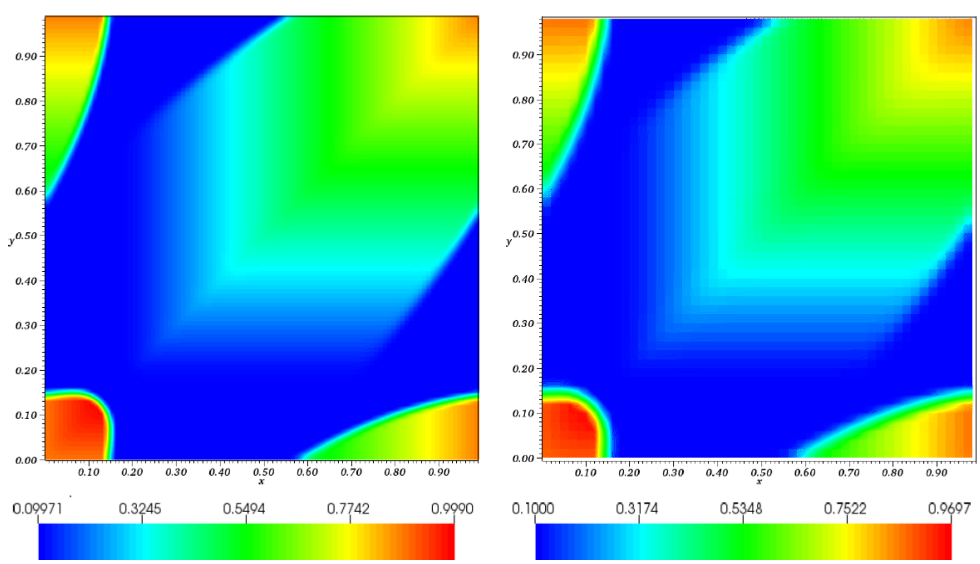

Figure 6: Numerial results for Burgers equation (velocity component u): reference solution (left) and SDPUS-C1 scheme (right).

In particular, we considered the shock-shock interaction problem, which consists of the interaction of two oblique shocks (states ⓐ and ⓒ) with two normal shocks (states ⓑ and ⓓ), described in figure 7. The problem is modeled by two-dimensional Euler equations defined on $[0,1]\times[0,1]$, supplemented with the initial conditions

$$[\rho_0, \quad u_0, \quad v_0, \quad p_0]^T = \begin{cases} [1.5, \quad 0, \quad 0, \quad 1.5]^T & \text{state ⓐ}, \\ [0.13799, \quad 1.2060454, \quad 1.2060454, \quad 0.0290323]^T & \text{state ⓑ}, \\ [0.5322581, \quad 1.2060454, \quad 0, \quad 0.3]^T & \text{state ⓒ}, \\ [0.5322581, \quad 0, \quad 1.2060454, \quad 0.3]^T & \text{state ⓓ}. \end{cases} \tag{22}$$

and zero-order extrapolation on the boundary.

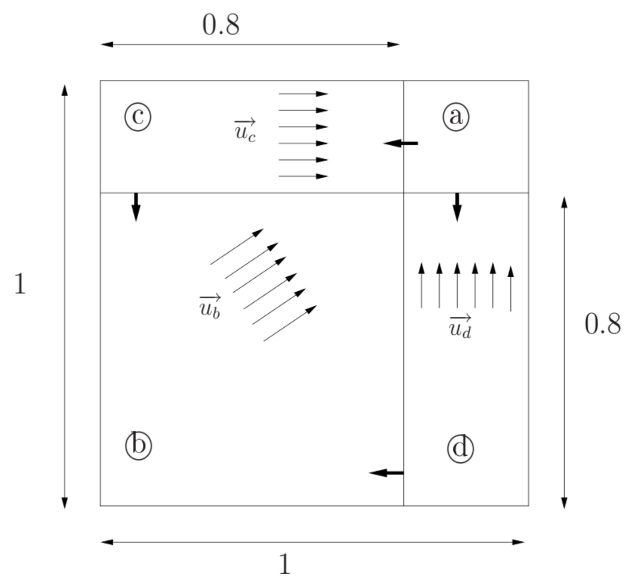

Figure 7: Schematic representation of the shock-shock interaction problem.

The reference solution is calculated using the Godunov method with a term of correction containing the MC flux-limiter of Leveque. The numerical solution is calculated by using the SDPUS-C1 in the version of the flux-limiter. Both the numerical and reference solutions were calculated on a mesh size of 200×200 computational cells and at $\theta = 0.8$. Figure 8 depicts the solutions for contours of the density profile at time $t = 0.8$. We also report in this same figure the distribution of the density along the diagonal ($y = x$). It can be clearly see from these figures that the SDPUS-C1 scheme solved well the complex structure in the solution.

4.3 Incompressible Navier-Stokes equations: free surface flows

From now on, we examine the capability of the SDPUS-C1 scheme to solve three-dimensional incompressible fluid flows involving moving free surfaces. The governing

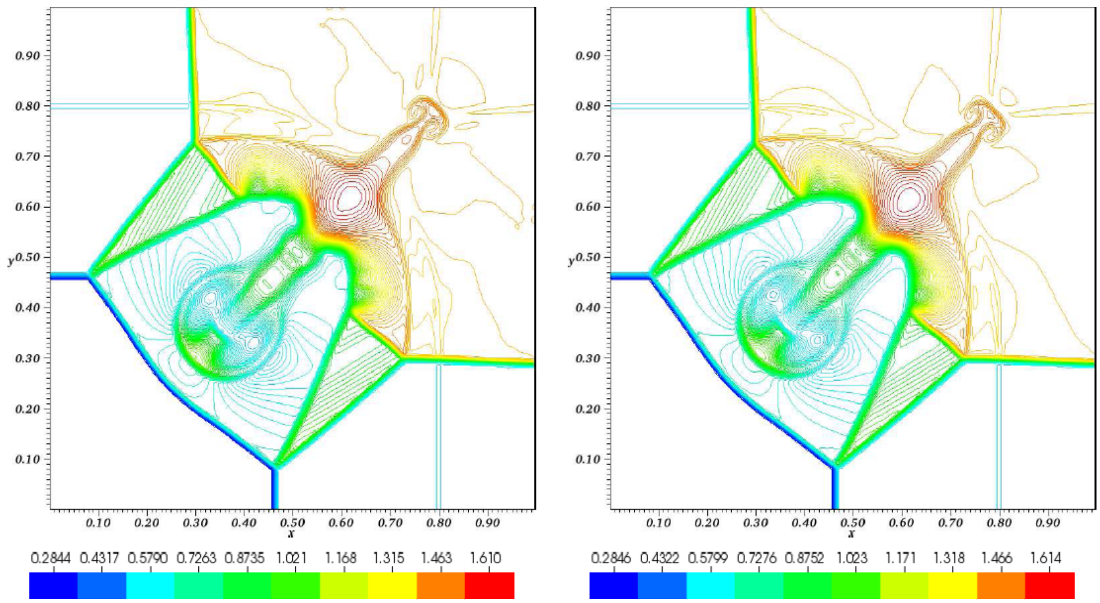

Figure 8: Numerial results for Euler equations (solutions in terms of contours of the density ρ): reference solution (left) and SDPUS-C1 scheme (right).

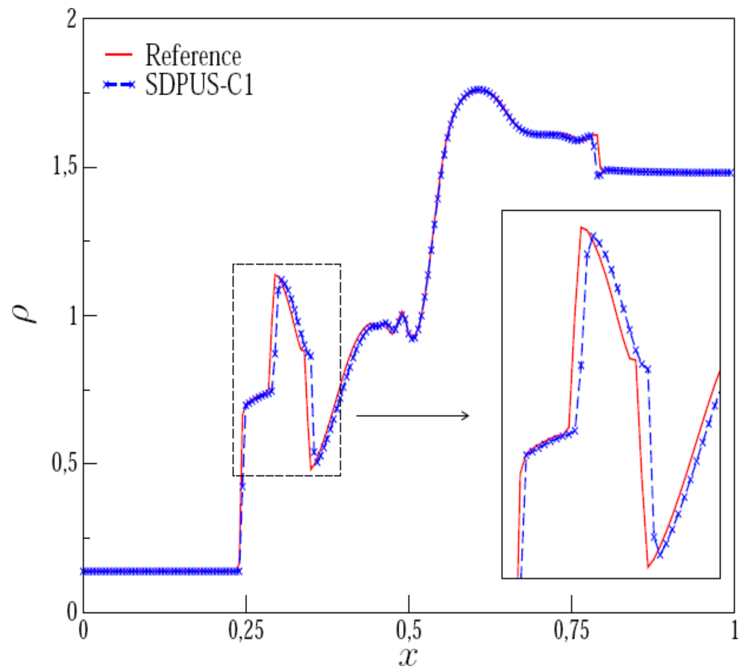

Figure 9: Numerial results for Euler equations (ρ on the line $y = x$).

equations are the full Navier-Stokes and mass conservation equations which, in Einstein notation, are given, respectively, by

$$\frac{\partial u_i}{\partial t} + \frac{\partial (u_i u_j)}{\partial x_j} = -\frac{\partial p}{\partial x_i} + \frac{1}{R_e}\frac{\partial}{\partial x_j}\left(\frac{\partial u_i}{\partial x_j}\right) + \frac{1}{F_r^2} g_i, \quad i = 1, 2, 3, \tag{23}$$

$$\frac{\partial u_i}{\partial x_i} = 0, \tag{24}$$

where u_i is i-th component of the velocity vector field, p is the pressure, and g gravitational field. The dimensionless parameters $Re = LV_0/\nu$ and $Fr = \frac{U_0}{\sqrt{L_0/g}}$ are the Reynolds and Froud numbers, respectively, with ν being the coefficient of viscosity (constant), L the lenght scale and V_0 the velocity scale.

We considered two well recognized complex test problems, namely, the circular hydraulic jump (see, for example, Ellegaard[5]) and jet buckling (see, for example, Nóbrega[15]). These are excellent tests for validation of numerical methods for computing fluid flow problems involving moving free surfaces. The three-dimensional version of the Freeflow code of Castelo et al.[2] equipped with the SDPUS-C1 scheme was employed in the computation. The numerical results are compared with experimental data.

4.3.1 Circular hydraulic jump

A hydraulic jump is a phenomenon familiar to everyone, when a water jet from a kitchen tap strikes a horizontal plate, an almost circular ring forms some distance away from the jet impact point (see figure 10). The ring is characterized by a sudden jump in the water depth (for more details, the reader can see Kasimov[10]).

Figure 10: Circular hydraulic jump.

In order to simulate this complex three-dimensional free surface flow, we considered an inflow section (the injector) of the diameter $D = 0.05m$, height $H = 0.001m$, and a mesh with $120 \times 120 \times 10$ computational cells. The rest of the data are as follows:

- Domain: $0.6m \times 0.6m \times 0.05m$;
- Gravitational constant: $g = 9.81m/s^2$;
- Lenght scale: $L = D = 0.05m$;
- Velocity scale: $V_0 = 1m/s$;
- Coefficient of viscosity: $\nu = 5 \times 10^{-5}m^2/s$;
- Reynolds number: $Re = \frac{V_0 \cdot L}{\nu} = 1000$;
- Froud number: $Fr = \frac{V_0}{\sqrt{g \cdot L}} = 1.4278$.

Figure 11 shows a qualitative comparison between the experimental results of Ellegaard et al.[5] and the results obtained with our numerical method equipped with the new upwind scheme. One can clearly see from this figure that our numerical method capture the complete physical mechanism of this complex three-dimensional free surface flow.

4.3.2 Jet buckling

The buckling of a fluid jet impinging onto a rigid wall is an interesting fluid mechanical instability with applications in food and polymer processing, geophysics, and many other areas. Applications of this low Reynolds number moving free surface flow have a long and distinguished history, dating back to Taylor[17].

Some authors, for example Bonito et al.[1], have considered the possibility of numerical methods for simulating this physical instability. Today, this problem provides an excellent test for validating numerical methods for highly viscous flows. Here, the SDPUS-C1 scheme is also tested in the simulation of the jet buckling problem.

To demonstrate that the numerical method presented here can cope with three-dimensional complex flows possessing an arbitrary free surface configuration, we simulated this flow by using the diameter of the injector $D = 0.006m$, height of the injector $H = 0.11m$, and a mesh with $100 \times 100 \times 100$ computational cells. Other data are:

- Domain: $0.06m \times 0.06m \times 0.11m$;
- Gravitational constant: $g = 9.81m/s^2$;
- Lenght scale: $L = D = 0.006m$;
- Velocity scale: $V_0 = 1m/s$;
- Coefficient of viscosity: $\nu = 1.2 \times 10^2 m^2/s$;
- Reynolds number: $Re = \frac{V_0 \cdot L}{\nu} = 0.5$;
- Froud number: $Fr = \frac{V_0}{\sqrt{g \cdot L}} = 4.12182$.

Experimental results of Ellegaard et al.

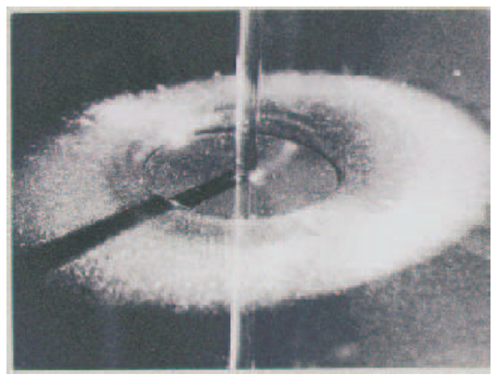

SDPUS-C1 scheme

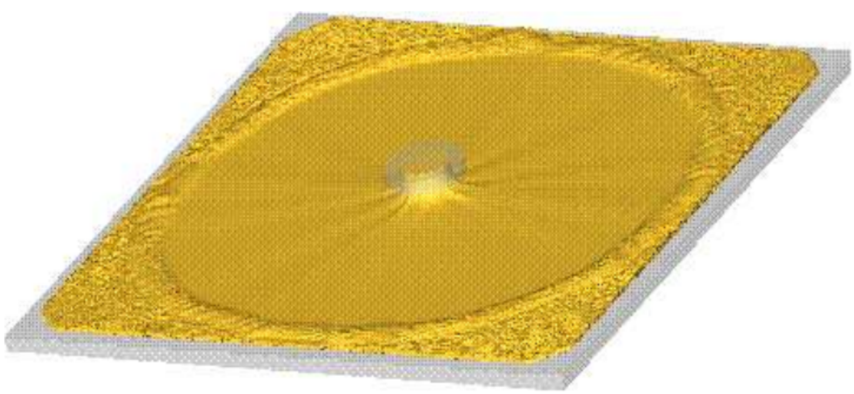

Figure 11: Results for a circular hydraulic jump problem.

Figure 12 shows the comparison of the result with SDPUS-C1 and the experiment by Nobrega et al.[15]. As one can see, the numerical results show that the buckling phenomenon can be captured with success by the SDPUS-C1 scheme.

Experimental results of Nóbrega et al.

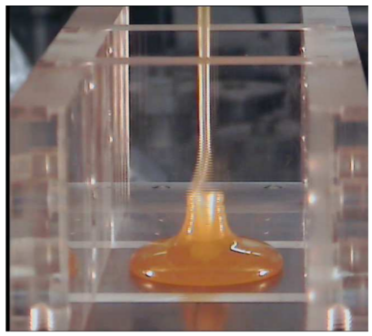

SDPUS-C1 scheme

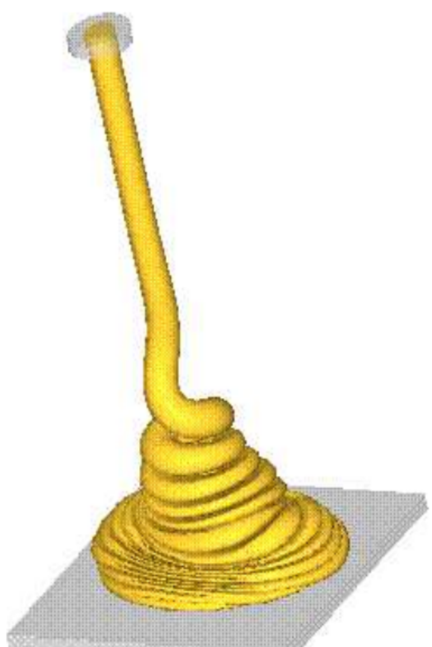

Figure 12: Results for the jet buckling problem.

5 CONCLUSIONS

In this paper, a high resolution polynomial upwinding scheme (SDPUS-C1) was presented for the numerical solution of time dependent conservation laws and related fluid dynamics problems. Various test problems formulated by two-dimensional conservation laws, such as, acoustics, Burgers and Euler equations were solved. And as an application, the SDPUS-C1 scheme was used to simulate of three-dimensional incompressible flows involving free surfaces. The results demonstrated that this upwinding scheme is an effective tool for studying these complex fluid dynamics problems. For the future, the authors are planning to apply SDPUS-C1 scheme to the numerical solution of three-dimensional turbulent viscoelastic free surface flows.

6 ACKNOWLEDGEMENTS

We gratefully acknowledge the support provided by FAPESP (Grants 2009/16954-8 and 2008/07367-9), CNPq (Grants 300479/2008-5 and 133446/2009-3) and CAPES (Grants PECPG1462/08-3).

REFERENCES

[1] A. Bonito, M. Picasso and M. Lasob, Numerical simulation of 3D viscoelastic flows with free surfaces, *Journal of Computational Physics*, **215** 691-716 (2006).

[2] A. F. Castelo, M. F. Tomé, C. N. L. César, S. Mckee and J. A. Culminato, Freeflow: an integrated simulation system for three-dimensional fre-surface flows, *Journal of Computers and Visualization in Science*, **2**, 199-210 (2000).

[3] R. Courant, E. Isaacson and M. Rees, On the solution of nonlinear hyperbolc differential equations by finite differences, *Community Pure Applied Mathematics*, **5**, 243-255 (1952).

[4] C. Cunha, Métodos Numéricos, 2th Edition, *Campinas/Brasil*, (2000).

[5] C. Ellegaard, A. e. Hansen, A. Haaning, K. Hansen, A. Marcussen, and T. Bohr, Poligonal hydraulic jumps, *Nonlinearity*, **12**, 1-7 (1999).

[6] V. G. Ferreira, R. A. Queiroz, G. A. B. Lima, R. G. Cuenca, C. M. Oishi, and S. McKee, An upwind differencing scheme for conservation laws and related fluid dynamics problems, *Computers & Fluids*, in review.

[7] V. G. Ferreira, M. K. Kaibara, G. A. B. Lima, J.M.Silva, M. H. Sabatine, P. F. A. Mancera, and S. McKee, A robust TVD/NV-based upwinding scheme for solving complex fluid flow problems, *International Journal for Numerical Methods in Fluids*, submitted.

[8] P. H. Gaskell and A. K. C. Lau, Curvature-compensated convective transport: smart, a new boundedness preserving transport algorithm, *International Journal for Numerical Methods in Fluids*, **8**, 617-641 (1988).

[9] A. Harten, High resolution schemes for hyperbolic conservation law, *Journal of Computational Physics* , **49**, 357-393 (1983).

[10] A. R. Kasimov, A stationary circular hydraulic jump, the limits of its existence and its gas dynamics anlogue, *Journla Fluid Mechanics*, **601**, 189-198 (2008).

[11] B. Leonard, Simple high-accuracy resolution program for convective modeling of discontinuities, *International Journal for Numerical Methods in Fluids*, **8**, 1291-1318 (1988).

[12] R. J. LeVeque, Finite volumes methods for hyperbolic problems, *Press Syncicate of the University of Cambridge*, (2004).

[13] G. A. B. Lima, Desenvolvimento de estratégias de captura de descontinuidades para leis de conservaćão e problemas realcionados em dinâmica dos fluidos, *Instituto de Ciências Matemáticas e de Computaćão, Universidade de São Paulo/Brasil*, (2010).

[14] H. Lin and C. C. Chieng, Characteristic-based flux limiters of an essentially third-order flux-splitting method for hyperbolic conservation laws, *International journal for Numerical Methods in fluids*, **13**, 563-565 (1991).

[15] M. Nóbrega, O. S. Carneiro, F. T. Pinho, G. S. Paulo, M. F. Tomé, A. Castelo and J. A. Culminato, The phenomenon of jet buckling: experimental results and numerical predictions, *Proceedings of The Polymer Processing Society 23rd Annual Meeting*, (2007).

[16] P. k. Sweby, A novel finite difference formulation for differential expressions involving both first and second derivatives, *SIAM Journal on Numerical Analysis*, **21**, 995-1011 (1884).

[17] G. I. Taylor, Low-Reynolds number flows, *National Commitee for Fluid Mechanics Films. Illustrated experiments in fluid mechanics*, (1974).

[18] N. P Waterson and H. Deconinck, Design principles for bounded higher-order convection schemes - a unified approach, *Journal of Computational Physics*, **224**, 182-207 (2007).